Contribution from the Departments of Chemistry and Physics, Karl-Marx-University, DDR-7010 Leipzig, GDR,
Department of Chemistry, University of Tromsö, N 9001 Tromsö, Norway, and Department of Molecular Spectroscopy,
Research Institute of Materials (RIM), University of Nijmegen, Toernooiveld, 6525 ED Nijmegen, The Netherlands

Crystal Structure and EPR/ENDOR Study of the Nonplanar System Bis(tetraphenylarsonium) Bis(maleonitriledithiolato)zincate(II) Doped with Copper(II)

J. Stach,[†] R. Kirmse,*[†] J. Sieler,[†] U. Abram,[†] W. Dietzsch,[†] R. Böttcher,[‡] L. K. Hansen,[§]
H. Vergoossen,[‖] M. C. M. Gribnau,[‖] and C. P. Keijzers*[‖]

Received August 5, 1985

A single-crystal EPR and ^{13}C ENDOR study on bis(tetraphenylarsonium) bis(maleonitriledithiolato)cuprate(II), $[(C_6H_5)_4As]_2[Cu(mnt)_2]$, and the crystal and molecular structure of the corresponding zinc host complex are reported. $[(C_6H_5)_4As]_2[Zn(mnt)_2]$ crystallizes in the monoclinic crystal system, space group $P2_1/c$, with $Z = 4$, $a = 17.559$ (3) Å, $b = 16.828$ (3) Å, $c = 18.542$ (2) Å, and $\beta = 110.43$ (1)°. The coordination of the Zn ion by the four sulfur atoms is almost tetrahedral. The angle between the ligand planes is 84°. From EPR and ENDOR measurements, the structure of the incorporated $[Cu(mnt)_2]^{2-}$ anions is determined. The themselves planar $[Cu(mnt)_2]^{2-}$ anions do not accept the structure of the host. Instead, an angle of 30° between the ligand planes has been found by EPR and of 30 or 46° with ^{13}C ENDOR on the ring-carbon atoms. Comparison of the experimental EPR parameters with the parameters that are computed from the results of extended Hückel molecular orbital calculations for various molecular geometries suggests an angle of approximately 30°. The EPR line width decreases exponentially with decreasing temperature, down to 150 K. It points to an activated process with an activation energy of 3.9 kcal/mol.

Introduction

Dithiolene ligands form square-planar transition-metal bis complexes,[1-5] but in recent years three interesting deviations from planarity were reported. The first case was published by Snaathorst et al.[6] for $(MB)_2[Cu(mnt)_2]$ (MB = methylene blue cation; mnt = maleonitriledithiolate), in which the mnt^{2-} ligands are rotated by 47°. The second one was claimed by Lundquist et al.,[7] who found for $[Ni(dmit)_2]^-$ (dmit = 2-thioxo-1,3-dithiole-4,5-dithiolate) an angle of 6.1° between the ligand planes. The third one is the $[(CH_3)_4N]_2Cu(mnt)_2$ complex, in which the dihedral angle between the ligand planes is 41°.[8] Up to now, X-ray structures of tetrahedrally coordinated dithiolene complexes have not been known.[9] Out of the group IIb (12[47]) elements, the Zn(II) ion prefers this coordination in the case of unsaturated dichalcogeno ligands like dithio- and diselenocarbamates.[10,11] Therefore, the presumption seemed to be justified that zinc(II) dithiolene chelates would be tetrahedral as well. In order to confirm this assumption, bis(tetraphenyl arsonium) bis(maleonitriledithiolato)zincate(II), $[(C_6H_5)_4As]_2[Zn(mnt)_2]$, was prepared and characterized by a crystal structure analysis.

Because of the uncommon structure, the complex is also an interesting host lattice for EPR and ENDOR measurements. Until now the guest complex $[Cu(mnt)_2]^{2-}$ has been investigated in planar host lattices[12-16] or in undiluted crystals.[6,17,18] If $[Zn(mnt)_2]^{2-}$ is the host, it is of special interest whether the guest accepts the tetrahedral structure because $[Cu(mnt)_2]^{2-}$ is planar by itself.

Besides the EPR behavior, ^{13}C ENDOR investigations are reported, because these proved to be helpful in understanding the bonding in some similar systems.[16,19,20] For the interpretation of the EPR/ENDOR results it turned out to be necessary to have an idea about the dependence of the experimental data on changes in the molecular structure. Therefore, the EPR parameters were calculated on the basis of an extended Hückel molecular orbital (EHMO) model for various molecular geometries.

Experimental Section

A. Preparation of Complexes and Single Crystals. Na_2mnt was prepared according to the method of Bähr and Schleizer.[21,22] The synthesis was performed with ^{13}C-enriched CS_2 (enrichment 35%)[23] in order to obtain mnt^{2-} complexes in which the chelate ring atoms are ^{13}C-labeled.

Yellow $[(C_6H_5)_4As]_2[Zn(mnt)_2]$ was prepared as described by Gray et al.[24] Brown $[(C_6H_5)_4As]_2[^{63}Cu(mnt)_2]$ was synthesized in the same manner with use of ^{63}Cu-enriched $CuCl_2 \cdot 2H_2O$ (97.8% ^{63}Cu, 2.2% ^{65}Cu). Green single crystals containing 2 mol % of the paramagnetic copper(II) complex were grown by slow solvent evaporation from acetone/ethanol (5:1) solution.

Table I. Fractional Positional Coordinates[a] of $[Zn(mnt)_2]^{2-}$

atom	*x*	*y*	*z*
Zn	0.76452 (5)	0.40878 (5)	0.05970 (5)
S_1	0.8445 (1)	0.2977 (1)	0.1134 (1)
S_2	0.6443 (1)	0.3355 (1)	0.0185 (1)
S_3	0.7787 (1)	0.5094 (1)	0.1507 (1)
S_4	0.7818 (1)	0.4937 (1)	−0.0318 (1)
C_1	0.7643 (4)	0.2347 (4)	0.1088 (4)
C_2	0.6837 (4)	0.2497 (4)	0.0689 (4)
C_3	0.7868 (4)	0.1636 (4)	0.1537 (4)
C_4	0.6249 (4)	0.1904 (4)	0.0682 (5)
C_5	0.7846 (3)	0.5876 (4)	0.0920 (4)
C_6	0.7854 (3)	0.5818 (4)	0.0192 (4)
C_7	0.7853 (4)	0.6652 (4)	0.1247 (4)
C_8	0.7833 (4)	0.6532 (5)	−0.0238 (4)
N_1	0.8070 (4)	0.1081 (4)	0.1913 (4)
N_2	0.5755 (4)	0.1449 (4)	0.0659 (5)
N_3	0.7843 (5)	0.7254 (4)	0.1530 (4)
N_4	0.7807 (4)	0.7081 (4)	−0.0608 (4)

[a] The standard deviation in the last digit is in parentheses.

[†] Department of Chemistry, Karl-Marx-University.

[‡] Department of Physics, Karl-Marx-University.

[§] University of Tromsö.

[‖] University of Nijmegen.

(1) McCleverty, J. A. *Prog. Inorg. Chem.* **1968**, *10*, 49.

(2) Schrauzer, G. N. *Transition Met. Chem. (N.Y.)* **1968**, *4*, 299.

(3) Eisenberg, R. *Prog. Inorg. Chem.* **1970**, *12*, 295.

(4) Hoyer, E.; Dietzsch, W.; Schroth, W. *Z. Chem.* **1971**, *11*, 41.

(5) Burns, R. P.; McAuliffe, C. A. *Adv. Inorg. Chem. Radiochem.* **1979**, *22*, 303.

(6) Snaathorst, D.; Doesburg, H. M.; Perenboom, J. A. A. J.; Keijzers, C. P. *Inorg. Chem.* **1981**, *20*, 2526.

(7) Lundquist, O.; Anderson, L.; Sieler, J.; Steimecke, G.; Hoyer, E. *Acta Chem. Scand., Ser. A* **1982**, *A36*, 855.

(8) Mahadevan, C.; Seshasayee, M. *J. Crystallogr. Spectrosc. Res.* **1984**, *14*, 215.

(9) During the preparation of this paper Greiwe et al. reported the structure of an almost tetrahedral Mn(II) dithiolene complex, $[(C_6H_5)_4P]_2[Mn(tdt)_2] \cdot 2CH_3OH$ (tdt = toluenedithiol): Greiwe, K.; Krebs, B.; Henkel, G. *Abstracts of Papers*, 23rd International Conference on Coordination Chemistry, Boulder, CO, 1984; Cooperative Institute for Research in Environmental Sciences, University of Colorado: Boulder, CO, 1984; p 54.

(10) Bonamico, M.; Dessy, G. *J. Chem. Soc. A* **1971**, 264.

(11) Bonamico, M.; Mazzone, G.; Vaciago, A.; Zambonelli, L. *Acta Crystallogr.* **1965**, *19*, 898.

(12) Maki, A. H.; Edelstein, N.; Davison, A.; Holm, R. H. *J. Am. Chem. Soc.* **1964**, *86*, 4580.

(13) White, L. K.; Belford, R. L. *J. Am. Chem. Soc.* **1976**, *98*, 4428.

(14) Kirmse, R.; Stach, J.; Dietzsch, W.; Hoyer, E. *Inorg. Chim. Acta* **1978**, *26*, L53.

(15) Inoue, M.; Hiroyoshi, K.; Nakamura, D. *J. Magn. Reson.* **1979**, *33*, 409.

(16) Kirmse, R.; Stach, J.; Abram, U.; Dietzsch, W.; Böttcher, R.; Gribnau, M. C. M.; Keijzers, C. P. *Inorg. Chem.* **1984**, *23*, 3333.

(17) Plumlee, K. W.; Hoffman, B. M.; Ratjack, M. T.; Kannenwurf, C. R. *Solid State Commun.* **1974**, *15*, 1651.

0020-1669/86/1325-1369$01.50/0

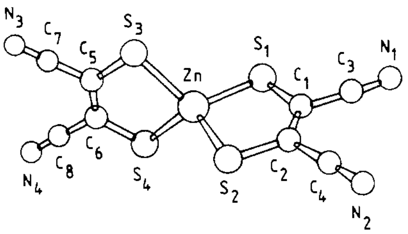

Figure 1. Numbering of the $[Zn(mnt)_2]^{2-}$ anion.

Table II. Bond Distances (Å) and Angles (deg)[a]

Zn–S_1	2.340 (2)	C_5–C_6	1.357 (8)
Zn–S_2	2.332 (1)	C_1–C_3	1.431 (8)
Zn–S_3	2.340 (2)	C_2–C_4	1.433 (8)
Zn–S_4	2.320 (2)	C_5–C_7	1.437 (8)
S_1–C_1	1.740 (5)	C_6–C_8	1.434 (9)
S_2–C_2	1.729 (6)	C_3–N_1	1.145 (9)
S_3–C_5	1.733 (6)	C_4–N_2	1.147 (8)
S_4–C_6	1.747 (6)	C_7–N_3	1.145 (9)
C_1–C_2	1.373 (7)	C_8–N_4	1.142 (9)
S_1–Zn–S_2	93.2 (2)	S_2–C_2–C_4	115.2 (4)
S_3–Zn–S_4	94.2 (2)	S_3–C_5–C_7	114.8 (4)
Zn–S_1–C_1	96.4 (1)	S_4–C_6–C_8	114.9 (4)
Zn–S_2–C_2	96.7 (2)	C_2–C_1–C_3	119.3 (5)
Zn–S_3–C_5	96.4 (2)	C_1–C_2–C_4	118.4 (5)
Zn–S_4–C_6	96.6 (1)	C_6–C_5–C_7	118.8 (5)
S_1–C_1–C_2	125.4 (4)	C_5–C_6–C_8	118.9 (5)
S_2–C_2–C_1	126.0 (4)	C_1–C_3–N_1	177.7 (6)
S_3–C_5–C_6	126.3 (4)	C_2–C_4–N_2	177.3 (7)
S_4–C_6–C_5	126.0 (4)	C_5–C_7–N_3	176.7 (7)
S_1–C_1–C_3	115.2 (4)	C_6–C_8–N_4	177.0 (7)

[a] The standard deviation in the last digit is in parentheses.

B. Intensity Data, Structure Determination, and Refinement. The intensity data of $[(C_6H_5)_4As]_2[Zn(mnt)_2]$ were collected on a CAD-4 diffractometer using Cu Kα radiation (λ = 1.54051 Å) monochromated with a graphite crystal monochromator. The unit cell dimensions were calculated from the setting angles of 25 reflections having $36° < 2\theta < 40°$. The complex crystallizes in the monoclinic crystal system, space group $P2_1/c$, with the cell constants $a = 17.559$ (3) Å, $b = 16.828$ (3) Å, $c = 18.524$ (2) Å, $\beta = 110.43$ (1)°, $V = 5127$ Å^3, $\rho_{calcd} = 1.44$ g cm^{-3}, and $Z = 4$.

A total of 11 100 reflections having $2° < \theta < 32°$ were recorded, from which 9748 were treated as observed ($I > 3.0\sigma(I)$). The intensities were corrected for Lorentz and polarization effects but not for absorption.

The Zn and S atoms were determined with use of the MULTAN program.[25] Refinement was made by full-matrix least-squares with anisotropic thermal parameters for all non-hydrogen atoms and isotropic thermal parameters for the hydrogen atoms. Hydrogen atom positions were calculated, and the final full-matrix refinement resulted in an R value of 0.068. The atomic scattering factors were taken from ref 48. All calculations were performed with use of the X-RAY 72 program.[26]

Lists of F_o/F_c, anisotropic thermal parameters of the non-hydrogen atoms, and the full set of positional coordinates have been deposited as supplementary material. The numbering of the anion is shown in Figure 1; the positional coordinates of the anion are given in Table I. Bond distances and angles of the $[Zn(mnt)_2]^{2-}$ anion are summarized in Table II.

C. EPR and ENDOR Measurements. Single-crystal EPR spectra were recorded at 295, 77, and 27.2 K on a Varian E-112 spectrometer at X-band frequency. The temperature dependence of the EPR line width was studied in the temperature range 4.2 K ≤ T ≤ 322 K.

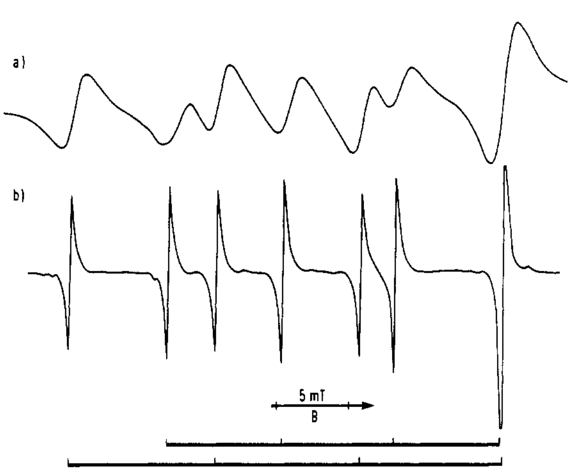

Figure 2. Typical EPR spectra of $[^{63}Cu/Zn(mnt)_2]^{2-}$ at T = (a) 295 and (b) 77 K.

The ENDOR investigations were performed with a modified Varian E-1700 spectrometer at 27.2 K. The low-power ENDOR apparatus is described elsewhere.[27]

The EPR-ENDOR spectra were recorded in three perpendicular planes every 10°. In order to correlate the measured EPR parameters with the crystal axes, the orientation of these axes with respect to the three rotation axes was determined with a CAD-4 diffractometer. The unit cell dimensions for the copper-doped crystal were found to be a = 17.70 Å, b = 16.94 Å, c = 18.64 Å, β = 110.1°, and V = 5247 Å^3, in good agreement with those obtained for the pure zinc(II) chelate.

Results and Discussion

A. Crystal Structure. The coordination of the zinc atom is almost tetrahedral. The angle between the least-squares planes through the ligands is 83.9°. Bends in the anion result in a very low symmetry. In contrast to the case for other dithiolene complexes,[17,18,24,28-30] the ligands themselves are not planar. The maximum deviation from the least-squares plane through the atoms Zn, S_1, S_2, C_1, and C_2 is 0.116 Å (S_1) and from the plane through the atoms Zn, S_3, S_4, C_5, and C_6 is 0.048 Å (S_4). The zinc–sulfur distances range from 2.32 to 2.34 Å. The geometry of the tetraphenylarsonium cations is tetrahedral, in agreement with earlier determinations.[31]

As mentioned already, nonplanarity is very uncommon for bis(1,2-dithiolene) complexes and $[(C_6H_5)_4As]_2[Zn(mnt)_2]$ represents the first authentic example of an almost tetrahedral one. Slight deviations from planarity seem to be a rule for dimeric dithiolene chelates in which the dimerization is based on intermolecular M–S bonds as was found for iron[32,33] and cobalt[34,35] complexes. On the other hand, the planarity remains if the dimerization is based on a metal–metal bond, as was observed for palladium and platinum complexes.[36] However, also in monomeric cobalt and iron dithiolene bis chelates with a third, monodentate ligand (phosphine, phosphine oxide, arsine, NO[37-39]) the metal atoms are located 0.2–0.5 Å above the basal plane of the sulfur atoms. Because of the presence of stereochemically

---

(18) Plumlee, K. W.; Hoffman, B. M.; Ibers, J. A.; Soos, Z. G. *J. Chem. Phys.* **1975**, *63*, 1926.
(19) Kirmse, R.; Abram, U.; Böttcher, R. *Chem. Phys. Lett.* **1982**, *88*, 98.
(20) Kirmse, R.; Abram, U.; Böttcher, R. *Chem. Phys. Lett.* **1982**, *90*, 9.
(21) Bähr, G.; Schleitzer, G. *Angew. Chem.* **1956**, *68*, 525.
(22) Bähr, G.; Schleitzer, G. *Chem. Ber.* **1957**, *90*, 428.
(23) Abram, U.; Kirmse, R.; Bubner, M. *Z. Chem.* **1982**, *22*, 216.
(24) Billig, E.; Williams, R.; Bernal, I.; Waters, J. H.; Gray, H. B. *Inorg. Chem.* **1964**, *3*, 663.
(25) Main, P. MULTAN 78, A System of Computer Programs for the Automatic Solution of Crystal Structures from X-ray Diffraction Data, Universities of York and Louvain-la-Neuve, 1978.
(26) "The X-ray System", Technical Report TR-192; Computer Science Center, University of Maryland: College Park, MD, June 1972.
(27) Böttcher, R.; Heinhold, D., submitted for publication in *Exp. Tech. Phys.*
(28) Fritchie, C. *Acta Crystallogr.* **1966**, *20*, 107.
(29) Kobayashi, A.; Sasaki, Y. *Bull. Chem. Soc. Jpn.* **1977**, *50*, 2650.
(30) Hove, M. J.; Hoffman, B. M.; Ibers, J. A. *J. Chem. Phys.* **1972**, *56*, 3490.
(31) Cowie, M.; Bennett, M. J. *Inorg. Chem.* **1976**, *15*, 1589.
(32) Hamilton, W. C.; Bernal, I. *Inorg. Chem.* **1967**, *6*, 2003.
(33) Schultz, A. J.; Eisenberg, R. *Inorg. Chem.* **1973**, *12*, 518.
(34) Enemark, J. H.; Lipscomb, W. N. *Inorg. Chem.* **1965**, *4*, 1729.
(35) Baker-Hawkes, M. J.; Dori, Z.; Eisenberg, R.; Gray, H. B. *J. Am. Chem. Soc.* **1968**, *90*, 4253.
(36) Browall, K. W.; Bursh, T.; Interrante, L. V.; Kasper, J. S. *Inorg. Chem.* **1972**, *11*, 1800.
(37) Rae, I. M. *Chem. Commun.* **1967**, 1245.
(38) Epstein, E. F.; Bernal, I. *J. Chem. Soc. D* **1970**, 136.
(39) Epstein, E. F.; Bernal, I. *Inorg. Chim. Acta* **1977**, *25*, 145.

Table III. Experimental[a] and Calculated Principal Values of $\bar{\bar{g}}$ and the Copper Hyperfine Tensor (10^{-4} cm^{-1}) and Directions of the Principal Axes (deg) in the Molecular Coordinate System

	exptl (T = 27.2, 77 K)				calcd			
	principal values	principal axes			principal values	principal axes		
		x	y	z		x	y	z
g_1	2.089	88	115	155	2.088	85	118	152
g_2	2.024	59	40	113	2.021	63	36	112
g_3	2.017	27	114	77	2.024	27	111	74
g_{av}	2.043							
$A_1 - A_{av}$	-62.1	89	116	154	-57.8	86	118	152
$A_2 - A_{av}$	27.6	44	53	110	30.8	48	47	107
$A_3 - A_{av}$	34.4	43	128	72	27.0	42	124	69
A_{av}	-47.9							

[a] Experimental errors: g_i, ±0.001; A_1, ±0.5; $A_{2,3}$, ±5.0.

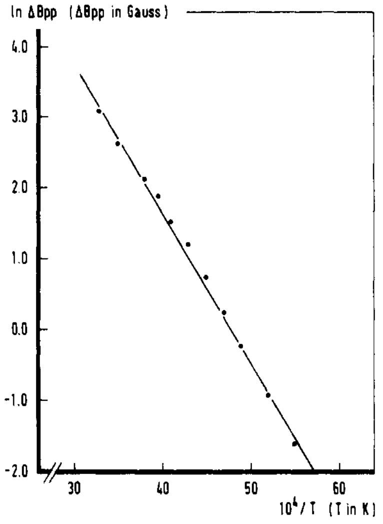

Figure 3. Width of EPR lines vs. temperature.

active lone pairs, the polymeric $[(C_6H_5)_4As][Bi(mnt)_2]$[40] and the monomeric $[(C_6H_5)_4As]_2[Te(mnt)_2]$[41] also do not have square-planar coordination, although the arrangement is quite different from tetrahedral.

B. EPR Investigations. In accord with the crystal structure of the host, the EPR spectra show two magnetically nonequivalent sites. At room temperature, the line width of each copper hyperfine line is unexpectedly large. Whereas for single-crystal spectra of similar copper complexes the line width varies between 0.25 and 0.40 mT, for the present system it was found to be ΔB_{pp} = 2.5 mT at 293 K. When the compound is cooled, the line width decreases continuously to 0.35 mT at 150 K and remains almost constant below that temperature down to 4.2 K. Spectra recorded at 295 and 77 K are shown in Figure 2. In Figure 3, the log of the line width is plotted vs. $1/T$. The linear relationship points to an activated process. The calculated activation energy is ~1880 K or 3.9 kcal/mol. In part E this line width behavior will be discussed in more detail, after the description of the EPR and the ENDOR results.

The spectra were analyzed with the computer program ESR64, which uses for this application[42] the spin Hamiltonian

$$\mathcal{H}_{sp} = \mu_B \vec{B}\cdot\bar{\bar{g}}\cdot\vec{S} + \vec{S}\cdot\bar{\bar{A}}^{Cu}\cdot\vec{I}^{Cu} + \vec{I}^{Cu}\bar{\bar{P}}^{Cu}\vec{I}^{Cu} - g_{Cu}\mu_N\vec{B}\cdot\vec{I}^{Cu} \qquad (1)$$

where $S = {}^1/_2$ and $I^{Cu} = {}^3/_2$. The program calculated transition energies and minimized the error function

$$h[(1/N)\sum_i^N(\nu^i_{obsd} - \nu^i_{calcd})^2]^{1/2} \qquad (2)$$

by varying the tensor elements of the Hamiltonian (1). In (2) i runs over all EPR peaks in all spectra of the same site. Both sites were measured and analyzed in the laboratory frame.

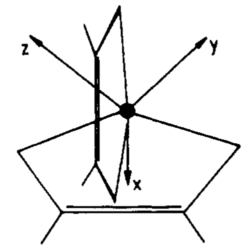

Figure 4. Molecular axis system.

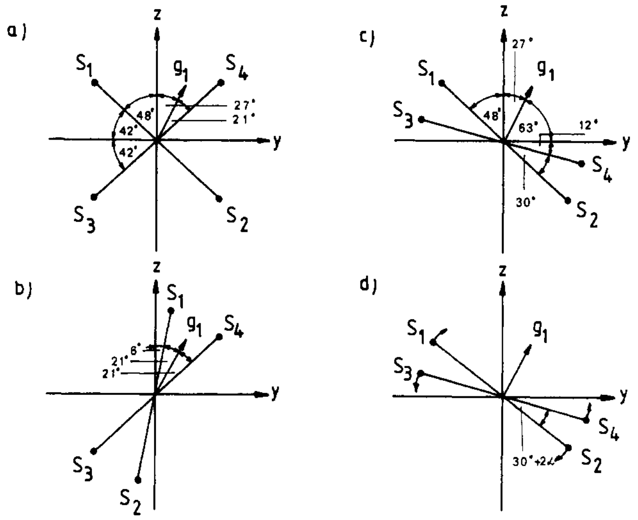

Figure 5. (a) Projection of the principal axis g_1 (A_1^{Cu}) in the yz plane of the molecular axis system with idealized planar ligands. (b–d) Possible ligand rotations.

For the interpretation of the measured tensors, it is necessary to transform them to the molecular axis system of the host complex (Figure 4). In this coordinate system the x axis bisects one of the ligands and the z axis is perpendicular to the least-squares plane through the zinc (copper) and the four sulfur atoms. It is not known which site belongs to which molecule in the unit cell. One of the two possible assignments resulted in arbitrary orientations of the tensor axes relative to the molecular axes. In the other assignment, the largest components of $\bar{\bar{g}}$ and $\bar{\bar{A}}^{Cu}$ of both sites are perpendicular to the molecular x axis. This assignment was taken to be the correct one, and the resulting tensor axes relative to the molecular axes are listed in Table III together with the principal values. Interestingly, these values at 27.2 and 77 K are equal to those measured at room temperature, within the experimental error, while, for instance, in the system $[Cu/Ni(mnt)_2]^{2-}$,[16] the principal values of $\bar{\bar{A}}^{Cu}$ are larger at liquid-neon temperature by about 5%.

Figure 5a shows a projection of the experimental g_1 (equal to the A_1^{Cu} axis) in the yz plane of the molecular system with idealized (planar) ligands. The angle between g_1, A_1^{Cu}, and the

---

(40) Hunter, C.; Weakly, T. J. R. *J. Chem. Soc., Dalton Trans.* **1983**, 1067.
(41) Golič, L.; Dietzsch, W., to be submitted for publication.
(42) For other applications of this program, see for instance: Paulissen, M. L. H.; Keijzers, C. P. *J. Mol. Struct.* **1984**, *113*, 267.

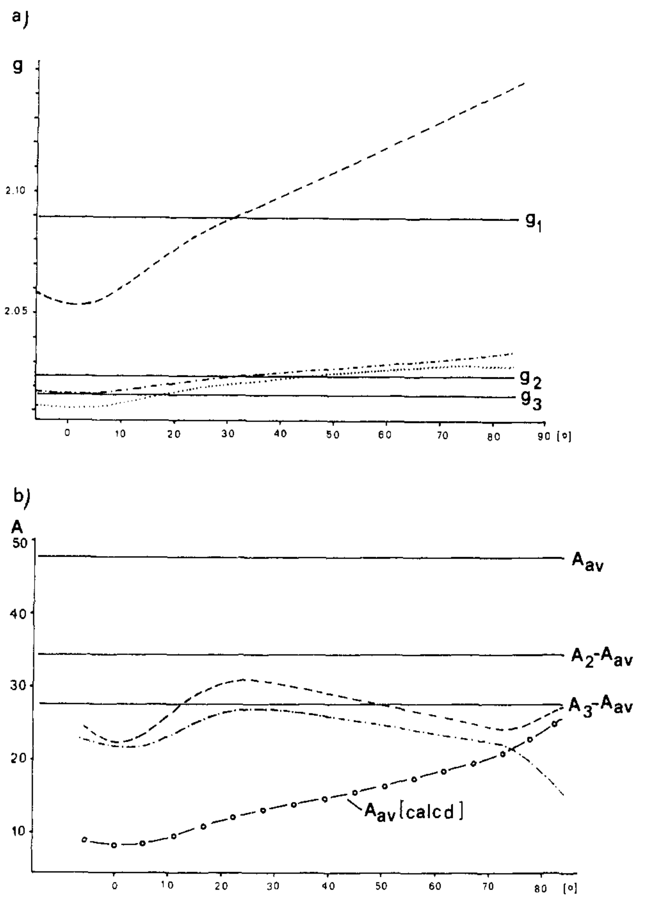

Figure 6. Calculated principal values of (a) $\bar{\bar{g}}$ and (b) $\bar{\bar{A}}^{Cu}$ as a function of the angle between the ligand planes. A_1 ($=-A_2 - A_3$) is not plotted. A_{av} is the isotropic value resulting from second-order contributions. Spin polarization is not taken into account. The experimental values are plotted as horizontal, solid lines.

molecular z axis is 27°. If the $[Cu(mnt)_2]^{2-}$ anions accept the structure of the host complex, it is to be expected that the maximum components of $\bar{\bar{g}}$ and $\bar{\bar{A}}^{Cu}$ are parallel with the z axis (being an approximate twofold axis). Therefore, the conclusion seems to be justified that the ligands of the copper-containing molecules are rotated relative to their positions in the host lattice. The g_1, A_1^{Cu} direction can be made a twofold axis by rotation of only *one* ligand: either S_1–S_2 (Figure 5b) (which is rejected as a possibility because g_1, A_1^{Cu} are expected to be perpendicular to the least-squares plane of the CuS_4 unit) or S_3–S_4 (Figure 5c). The latter rotation results in an angle of 30° between the ligand planes. It is possible that, on top of this rotation, the two ligands are rotated in opposite directions over an angle α (Figure 5d). α may vary between −15° (planar geometry) and +30° (tetrahedron). These possibilities cannot be distinguished by means of the EPR measurements. The results of the ENDOR measurements and the MO calculations, on the other hand, do depend on this angle, and this will yield a solution (see below).

A more detailed picture of the structure of the $[Cu(mnt)_2]^{2-}$ guest molecules would be obtained if the ^{33}S hyperfine splittings could be measured. However, because of the low natural abundance of this isotope (0.74%, $I = {}^3/_2$) and the low symmetry of the copper complexes every copper hyperfine line is flanked by four quartets of ^{33}S satellites with an intensity of only 0.2% of the copper lines. Due to this low intensity and the many line overlappings it was not possible to determine the ^{33}S tensors.

C. Extended Hückel Molecular Orbital Calculations. In order to substantiate the conclusions about the structure of the $[Cu(mnt)_2]^{2-}$ guest molecules, EHMO calculations were performed. The MO's and energies and from them the $\bar{\bar{g}}$ and $\bar{\bar{A}}^{Cu}$ tensors were calculated for various angles between the ligand planes. The values for the empirical parameters and the basis set were taken from the calculations on bis(diethyldithiocarbamato)copper(II).[42,43]

Figure 7. ^{13}C ENDOR spectrum.

Table IV. Experimental Hyperfine Coupling Tensors of ^{13}C in the Molecular Frame (10^{-4} cm^{-1})[a]

		principal values	principal axes		
			x	y	z
C_a	A_1	−1.09	97	123	146
	A_2	−0.46	52	54	121
	A_3	−0.37	37	123	75
	A_{av}	−0.64			
C_b	A_1	−1.38	98	73	161
	A_2	−0.72	46	50	109
	A_3	−0.66	43	132	84
	A_{av}	−0.92			
C_c	A_1	−1.51	60	98	31
	A_2	−1.10	150	94	61
	A_3	−0.66	92	171	99
	A_{av}	−1.09			
C_d	A_1	−1.39	68	148	112
	A_2	−0.99	22	72	78
	A_3	−0.43	96	114	25
	A_{av}	−0.94			

[a] Experimental error: A_i, ±0.010.

The EPR parameters were calculated with the formulas derived in ref 43 and 44.

For the calculation of the planar $[Cu(mnt)_2]^{2-}$ anion, D_{2h} symmetry was assumed. The MO of the unpaired electron has B_{1g} symmetry and consists of the $3d_{xy}$ orbital of copper and hybrids of 3s, $3p_x$, and $3p_y$ orbitals of the sulfur atoms. When the ligands are twisted, the symmetry is lowered to D_2 and the MO of the unpaired electron becomes B_1. This results in three different causes for changes in the magnitude of $\bar{\bar{g}}$ and $\bar{\bar{A}}^{Cu}$: (1) mixing of the p_z orbitals of copper and sulfur in the MO of the unpaired electron, (2) changes in the excitation energies, and (3) changes in the delocalization upon rotation of the ligands.

Figure 6 shows the calculated total variation of the principal values of $\bar{\bar{g}}$ and $\bar{\bar{A}}^{Cu}$ for various angles between the ligand planes. It should be noted that the tensors are unreliable for angles close to 90°, because then the ground state is almost degenerate and the tensors are calculated with nondegenerate perturbation theory. The values calculated for an angle of 30° between the ligand planes give the best fit with the experimental values. They are listed in Table III. The maximum components of $\bar{\bar{g}}$ and $\bar{\bar{A}}^{Cu}$ make an angle of 28° with the z axis, also in good agreement with experiment. The calculated ^{33}S hyperfine structure tensors are not listed in Table III. They are $A_\parallel \approx 7.9 \times 10^{-4}$ cm^{-1}, $A_\perp \approx -4.0 \times 10^{-4}$ cm^{-1} and $A_{av} \approx 7.5 \times 10^{-4}$ cm^{-1}.

D. ENDOR Investigations. The ^{13}C ENDOR transitions were observed in the frequency range 1–6 MHz. Each ^{13}C nucleus ($I = {}^1/_2$) gives rise to two ENDOR transitions, and since all ring positions are ^{13}C-enriched and the symmetry of the $[Cu(mnt)_2]^{2-}$ anions is very low, 4 × 2 ^{13}C ENDOR transitions are expected. However, only the four high-frequency lines were observed without difficulty. The intensity of the low-frequency lines is reduced so drastically that they could be observed in a small frequency range only. ^{13}C atoms in natural abundance could not be detected. A typical spectrum is shown in Figure 7. The line width is about 40 kHz; the accuracy of the transition frequencies is about 20 kHz. The ENDOR data were treated for each ^{13}C nucleus individually with the program ESR64, which uses for this application the spin Hamiltonian (1), but extended with the hyperfine coupling and

---

(43) Keijzers, C. P. Ph.D. Thesis, University of Nijmegen, 1974.
(44) Keijzers, C. P.; de Boer, E. *Mol. Phys.* **1975**, *29*, 1007.

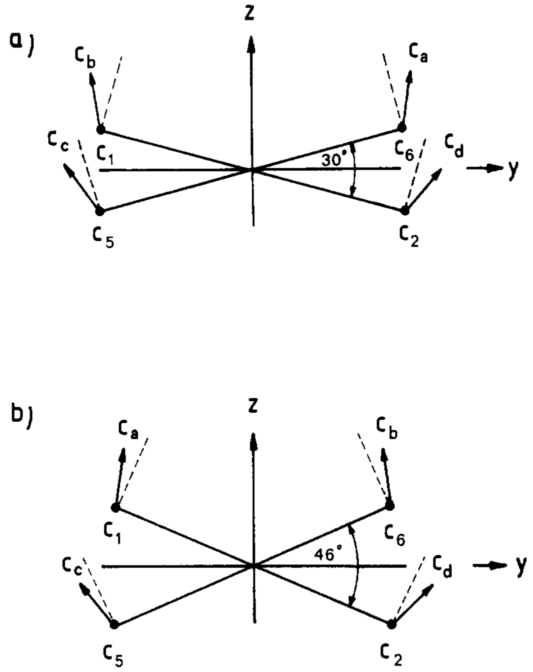

Figure 8. Assignment of the ^{13}C hyperfine tensors: (a) $C_a = C_6$, $C_b = C_1$, $C_c = C_5$, $C_d = C_2$; (b) $C_a = C_1$, $C_b = C_6$, $C_c = C_5$, $C_d = C_2$.

nuclear Zeeman energy of ^{13}C. The resulting hyperfine tensors in the molecular axis system are listed in Table IV. Note that the indices of the carbon atoms in this table are totally arbitrary.

For the assignment of the four tensors to the corresponding carbon atoms it was assumed that they will have the same orientation *relative to their own local axis system* but, of course, a different orientation relative to the molecular frame. There are two assignments to reach this situation (see Figure 8)

$$C_a = C_6,\ C_b = C_1,\ C_c = C_5,\ C_d = C_2 \qquad \text{(I)}$$

$$C_a = C_1,\ C_b = C_6,\ C_c = C_5,\ C_d = C_2 \qquad \text{(II)}$$

which result in angles of 30 and 46° between the ligand planes, respectively. In both cases the yz projections are identical for all four carbon atoms. The xz projections of the largest hyperfine tensor components are not identical for the idealized planar ligands. This is improved if the real structure of the host complex is used.

Concluding, one may say that EPR and ENDOR studies combined with EHMO calculations provide a detailed insight into the structure of the $[Cu(mnt)_2]^{2-}$ guest molecules incorporated in the $[Zn(mnt)_2]^{2-}$ host lattice. The copper complex has a structure between planar (pure $[Cu(mnt)_2]^{2-}$) and tetrahedral(host lattice), close to the structures of $(MB)_2Cu(mnt)_2$[6] and $[(CH_3)_4N]_2Cu(mnt)_2$.[8] The following results were obtained for the angle between the ligand planes: EPR shows rotation of one ligand over 30° $[S_3-S_4)$ and possibly a subsequent rotation of both ligands, ENDOR gives the solution 30 or 46°, and the EHMO calculations suggest an angle of approximately 30°. Therefore, it seems safe to conclude that the angle is 30° caused by the rotation of one ligand only. As shown by the ENDOR investigations, the ligands are not planar and have a structure close to that of the mnt^{2-} ligands of the host complex.

E. Temperature Dependence of the EPR Line Width. The relevant experimental observations are as follows: (1) the temperature dependence is exponential with an activation energy of ~1880 K (Figure 4); (2) the line width at room temperature is independent of the angle; (3) the lines are Lorentzian; (4) they do not shift with the temperature. The nature of the excited state is not known, but, because this is the first system among many similar ones[45] in which this effect is found and because this is also the first among these systems in which the guest structure is very different from that of the host, it seems logical to conclude that the two are related. It is proposed that in the excited state the ligand that deviates from the host structure is rotating around the x axis over an unknown but presumably small angle. Even if this would cause an inhomogeneous broadening, the line centers would not shift, because both **g** and A^{Cu} vary linearly with the rotation angle *around the low-temperature geometry of ~30°* (Figure 6). From the observations that the lines are Lorentzian and that their width is independent of the magnetic field angle (whereas the calculated **g** and A^{Cu} dependence on the ligand angle does depend on the magnetic field angle (Figure 6)), it is concluded that the line broadening is due to T_2 relaxation caused by the presence of the excited state. This homogeneous broadening may be described with the equations of Swift and Connick[46] for two-site problems with one of the populations being very low (as is the case for this excited state in the temperature range studied). The temperature-dependent part for the relaxation rate may be written as

$$\frac{1}{T_2(T)} = \left[\exp\left(\frac{-\Delta E}{kT}\right)\right]\frac{1}{\tau_b}\,\frac{\dfrac{1}{T_{2b}}\left(\dfrac{1}{T_{2b}}+\dfrac{1}{\tau_b}\right)+\Delta\omega_b^{2}}{\left(\dfrac{1}{T_{2b}}+\dfrac{1}{\tau_b}\right)^{2}+\Delta\omega_b^{2}} \qquad (3)$$

where ΔE is the activation energy, τ_b the lifetime of the excited state, T_{2b} its transverse relaxation time, and $\Delta\omega_b$ the difference between its resonance frequency and the microwave frequency. With use of observation 4, $\Delta\omega_b = 0$, eq 3 yields $T_{2b} + \tau_b \approx 3 \times 10^{-11}$ s, which implies that the relaxation time and the lifetime of the excited state must be extremely short. Therefore, further studies on the exact nature of this excited state will be very difficult or impossible.

Acknowledgment. We wish to thank Prof. Dr. L. Golič for determining the crystal axes of the $[(C_6H_5)As]_2[^{63}Cu/Zn(mnt)_2]$ crystal used for the EPR and ENDOR investigations and Dipl.Ing. D. Heinhold for his help in performing the ENDOR measurements.

Registry No. $[(C_6H_5)_4As]_2[Zn(mnt)_2]$, 101078-22-2; $[(C_6H_5)_4As]_2[Cu(mnt)_2]$, 101078-23-3.

Supplementary Material Available: Tabulations of observed and calculated structure factors and anisotropic thermal parameters of non-hydrogen atoms and full sets of positional coordinates and interatomic distances (54 pages). Ordering information is given on any current masthead page.

---

(45) Böttcher, R.; Kirmse, R.; Stach, J.; Keijzers, C. P. *Mol. Phys.* **1985**, *55*, 1431 and references therein.

(46) Swift, T. J.; Connick, R. E. *J. Chem. Phys.* **1962**, *37*, 307.

(47) The periodic group notation in parentheses is in accord with recent actions by IUPAC and ACS nomenclature committees. A and B notation is eliminated because of wide confusion. Groups IA and IIA become groups 1 and 2. The d-transition elements comprise groups 3 through 12, and the p-block elements comprise groups 13 through 18. (Note that the former Raman number designation is preserved in the last digit of the new numbering: e.g., III → 3 and 13.)

(48) *International Tables for X-ray Crystallography*; Kynoch: Birmingham, England, 1974; Vol. IV.